# Study on forging process and die design of parking sensor shell

*Tung-Sheng* Yang* and *Jhong -Yuan* Li

Department of Mechanical Manufacturing Engineering, National Formosa University,

64 Wunhau Road, Huwei, Yunlin, Taiwan 632, ROC

**Abstract.** The process of precision forging has been developed recently because of its advantages of giving high production rates and improved strength. For complete filling up, predicting the power requirement and final shape are important features of the forging process. A finite element method is used to investigate the forging force, the final shape and the stress distribution of the parking sensor shell forging. The stress-strain curve of AL-6082 is obtained by the computerized screw universal testing machine. The friction factor between AL-6082 alloy and die material (SKD11) are determined by using ring compression test. Stress-strain curve and fiction factor are then applied to the finite element analysis of the parking sensor shell forging. Maximum forging load, effective stress distribution and shape dimensions are determined of the parking sensor shell forging, using the finite element analysis. Then the parking sensor shells are formed by the forging machine. Finally, the experimental data are compared with the results of the current simulation for the forging force and shape dimensions of the parking sensor shell.

## 1 Introduction

Parking sensors are proximity sensors for road vehicles designed to alert the driver to obstacles while parking. These systems use ultrasonic sensors to proximity detectors to measure the distances to nearby objects via sensors located in the front or rear bumper fascia or visually minimized within adjacent grills or recesses. Manufacturing 3C products by applying cold bulk forming processes is a common production technique owing to its well-known advantages, such as reduced material and time costs and the resulting increased strength of the products. Moreover, the applications of cold forged aluminum alloy parts have been increasing because of the important needs for weight reduction of automobile. However the associated process planning and tool design are complex tasks.

The finite element method (FEM) is one of the most powerful tools of computer aided engineering (CAE) to solve various problems in metal forming processes. Commercial CAE software finds use in the areas of process verification and modification as well as for design improvement [1, 2, 3]. Aluminum alloys have been widely used to manufacture lightweight automotive bodies and parts. Jensrud et al. [4] proposed a new thermo-mechanical process for aluminum forging. They showed that it is possible to reduce the

Corresponding author: tsyang@nfu.edu.tw

load without reduction of the hardness under the proposed optimum processing conditions. Khaleed et al. [5] performed three-dimensional analysis including thermal effects for a flash-less cold forging product of aluminum alloy. They obtained a good agreement with experimental results and optimized the initial shape of the workpiece. The ring compression test has proven to be one of the most popular and commonly used methods for quantitative evaluation of friction conditions in bulk forming operations. The ring compression test was firstly used by Kunogi [6] as a qualitative method of comparing lubricants for cold extrusion. Lee and Altan [7] used an upper-bound velocity field that considers bulging has been applied to cylinder and ring upsetting. According to the relationship between inner diameter changes and height reduction, the calibration curve of constant shear friction factor for a 6:3:2 rings have been predicted.

This study development the aluminum alloy forging process and die design of parking sensor shell. The stress-strain curve of AL-6082 is obtained by the universal testing machine. The friction factor between AL-6082 and die material are determined by using ring compression test. Stress-strain curve and fiction factor are then applied to the finite element analysis of the parking sensor shell forging to predict the forging force and the shape of parking sensor. The experimental data are compared with the results of the current finite element simulation

## 2 Flow stress and friction factor of 6082 aluminum alloy

The computerized screw universal testing machine is used to determine the mechanical properties. A tensile specimen is a standardized sample cross-section. It has two shoulders and a gauge section in between. The shoulders are large so they can be readily gripped, whereas the gauge section has a smaller cross-section so that the deformation and failure can occur in this area. Figure 1(a) shows the dimensions of the tensile specimen. The tested tensile specimen is AL 6082 alloy. The test process involves placing the test specimen in the testing machine (Fig. 1(b)) and slowly extending it until the test specimen fractures (Fig.2(a)). During this process, the elongation of the gauge section is recorded against the applied force. The data is manipulated so that it is not specific to the geometry of the test sample. Thus the stress-stain curves and fracture values of AL 6082 alloy are obtained. Figure 2(b) presents the stress-stain curves of AL 6082 alloy at room temperature. To obtain the shear friction factor, the specimens are produced outer diameter, inner diameter and height as 18mm, 9mm and 6mm (6: 3: 2), respectively. The ring specimens are compressed with different deformation and lubricants. Fig. 3(a) shows the results of ring compression test. Both the reduction ratio of height and reduction ratio of inner diameter are calculated. Fig. 3(b) presents the friction factors of five specimens are between 0.10-0.15, and the average value of friction factor is about 0.13.

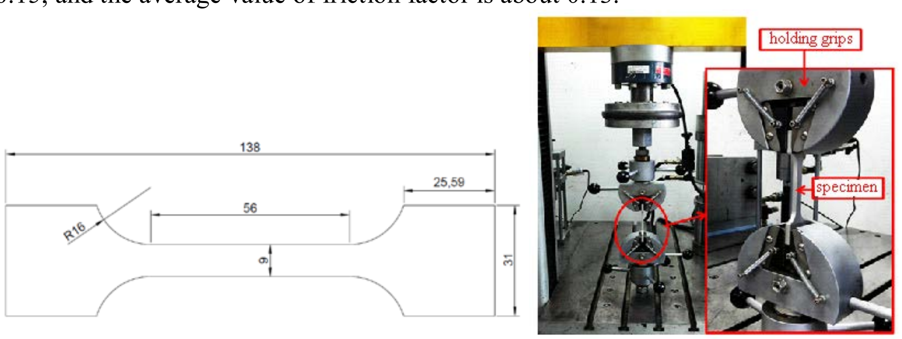


(a) Dimensions of the tensile specimen (b) Tested tensile specimen

**Fig. 1.** Dimensions of the tensile specimen and tested tensile specimen.

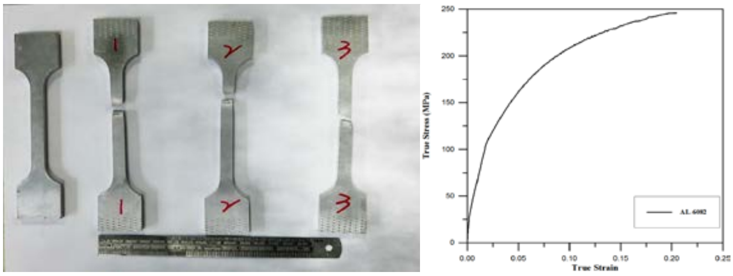


(a) Fractured specimen (b) True stress-stain curve

**Fig. 2.** fractured specimen and true stress-stain curve.

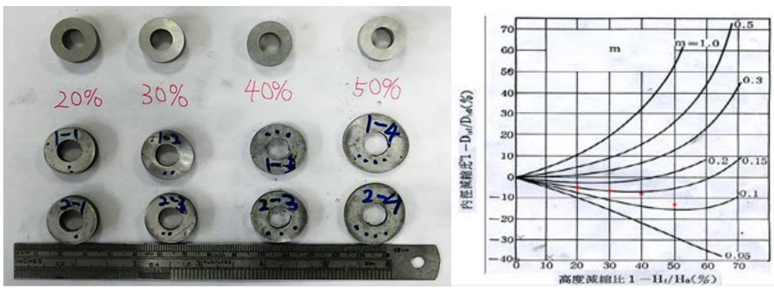


(a) Results of ring compression test (b) Friction factors of the specimens

**Fig. 3.** Results of ring compression test and friction factors of the specimens.

## 3 Finite element analysis of forging of parking shell

### 3.1 Production and die design

The parking sensor shell is mainly assembled with the mating sensor. Thus the shape of the sensor is used to determine the inner groove of the shell. Figure 4 shows the parking sensor assembly which include the sensor and shell. The top of the shell must to be fairly flat so that the ultrasonic transmission can accurately receive. In addition, due to the requirement of the parallelism, verticality and concentricity the further machining is needed after forging. Therefore the design of forged shell must take into account of machining allowance (about 0.3 mm) from the product design of shell. Figure 5 shows the product design of parking sensor shell. Forging dies include punch, die and other parts as shown in Fig. 6. The ejector rod is used to eject the forged piece from the die. Figure 7 shows the schematic diagram of the punch and die.

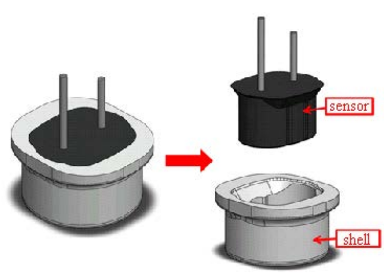


**Fig. 4.** Parking sensor assembly diagram (including sensor and shell).

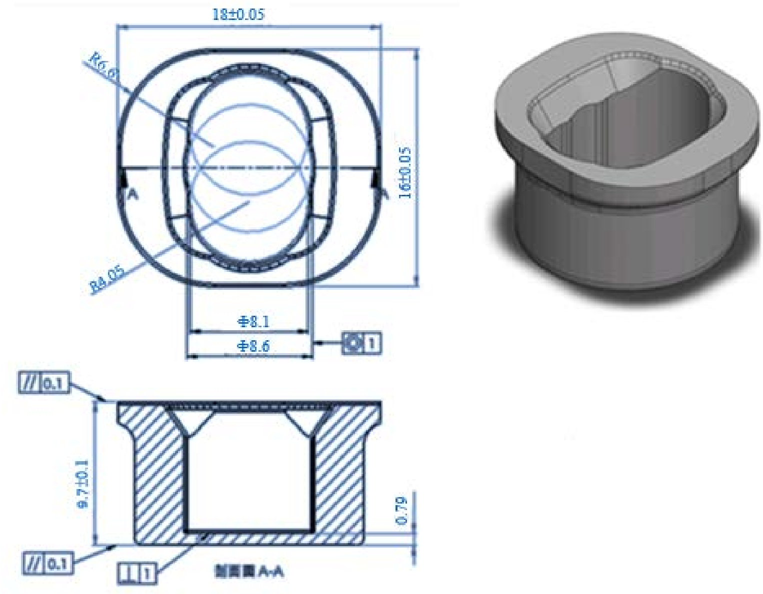


**Fig. 5.** Diagram of product design of parking sensor shell.

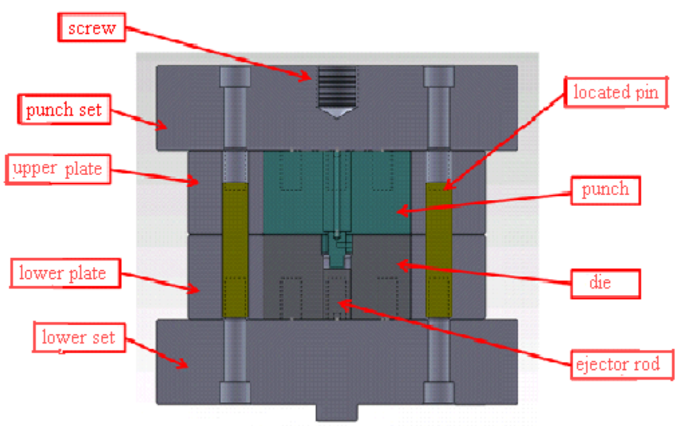


**Fig. 6.** Forging dies.

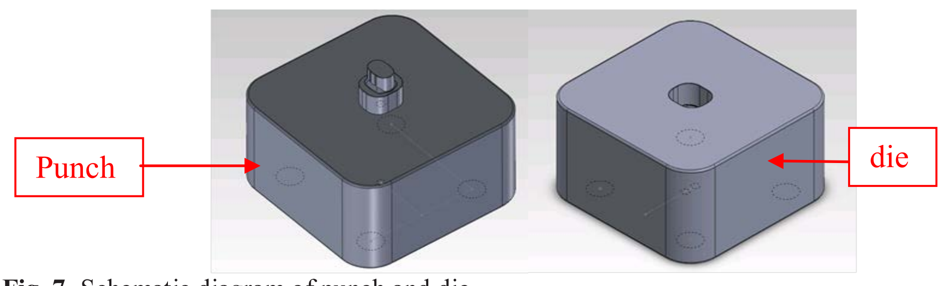


**Fig. 7.** Schematic diagram of punch and die.

### 3.2 Finite element analysis.

The FEM software DEFORM-3D [6] has been applied to simulate the plastic flow of materials during the forging process of parking sensor shell. The flow stress curves are the input data during the simulation of forging process. In addition to material properties, preprocessor also require input of detailed process parameters such as friction factor, punch velocity, dimensions of billet, etc. Figure 8 shows the schematic diagram of the parking sensor shell forging. The material is formed by the punch and the consequence the billet material flows into the shape of die. During the analyses, the die and the punch are assumed to be rigid, whereas the billet is assumed to be plastic. The flow stress of AL6082 billet obtained by universal testing machine is shown in Fig. 2(b). The constant friction factor is assumed as 0.13 at the interface between the billet and die. The value of friction factor is obtained by the ring compression test. The diameter and the height of billet are 15 mm and 6 mm, respectively. During the parking sensor shell forging simulation the element number of the billet is assumed as 80000-180000. When the element numbers exceed 140000 the forging force approach to a steady value about 190 tons (Fig. 9). Thus the element number is assumed as 140000. The details of simulation parameters are shown in Table 1.

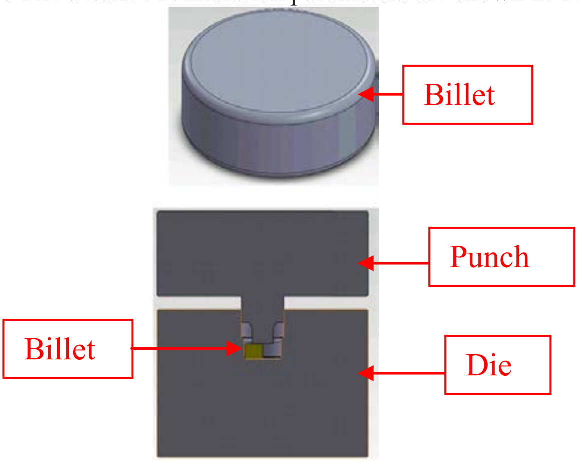


**Fig. 8.** Schematic diagram of parking sensor shell forging.

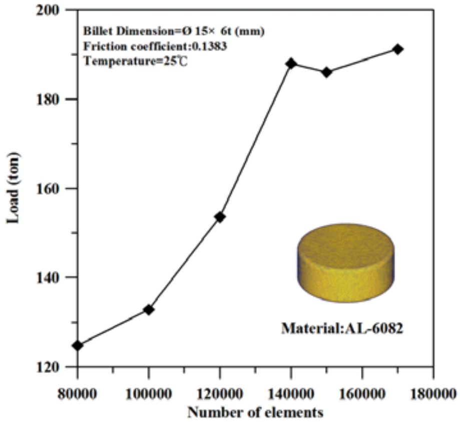


**Fig. 9.** Effect of number of elements on forging load.

 https://doi.org/10.1051/matecconf/201818500020

**Table 1.** Details of simulation parameters.

| | |
|---|---|
| friction factor | 0.13 |
| temperature (°C) | 25 |
| punch speed (mm/min) | 10 |
| billet dimension (mm) | Ø15 x 6 t |
| max. forging force (ton) | 188 |

Figure 10 shows the variation of the punch loads with punch stroke. The punch load increases as the punch stroke increases. When the material flows into the die cavity completely, the punch load increases rapidly, the maximum forging load is about 188 tons. Figure 11 shows the effective stress distribution of billet when the material flows into the die cavity completely. The maximum value of effective stress occurs at the fillet of die. Figure 12 shows the simulated shape of parking sensor shell.

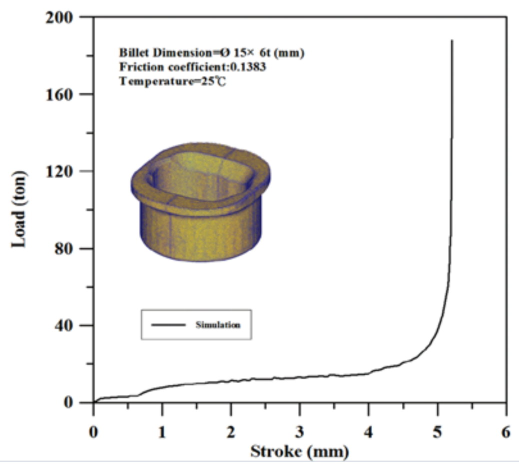


**Fig. 10.** Variation of the punch loads with punch stroke.

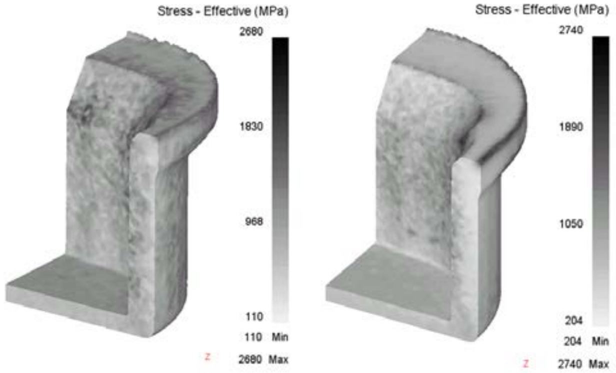


**Fig. 11.** Effective stress distribution of billet.

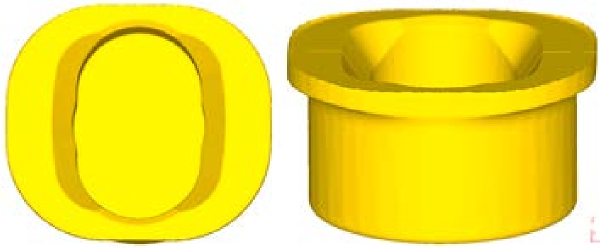

**Fig. 12.** Simulated shape of parking sensor shell.

## 4 Experimental results

Figure 13 shows the device of experiment including the forging machine, punch, die and guide pins. Guide pins are used to locate the movement of the upper and lower die. The test machine is 200 tons hydraulic test equipment, the forming speed is 10mm/min. The billet placed between punch and die. The material of billet is AL6082, and the material of die is SKD11. The diameter of billet is 15 mm, and the height of billet is 6 mm. The lubricant used in current experiment between die and billet is graphite, which is also used in the ring compression test. The die is stationary and the punch moved toward to the die until the material flow into the die cavity completely. Figure 14 shows the experimental result of forging the parking sensor shell. The experimental shape of parking sensor shell is near the simulated result which shown in Fig. 12. The dimensions of forged part are larger than the designed dimensions as shown in Fig. 5 about 0.30 mm, which is machining allowance of the product design of shell. The experimental punch load (about 191tons) agrees well with the simulation result (188 tons).

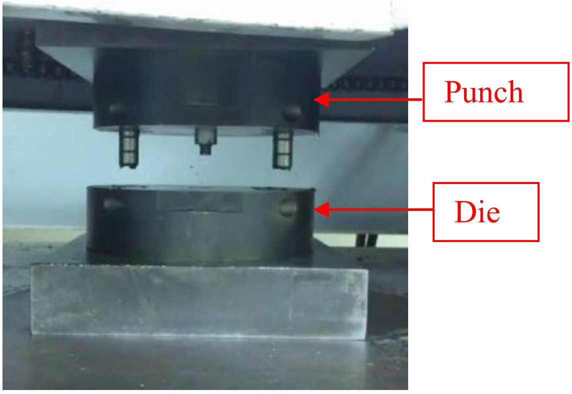


**Fig. 13.** Device of experiment (punch, die and guide pins).

**Fig. 14.** Experimental result of parking sensor shell.

## 5 Conclusions

The stress-strain curves of the AL6082 are obtained by the universal testing machine. The friction factor between the die and billet is obtained by ring compression test with different deformation and lubricant. The lubricant is graphite and the experimental friction factor is 0.13. Therefore the stress-strain curves and experimental friction factor are as the input parameters during the finite element analysis of parking sensor shell forging process. Maximum forging load, effective stress and shape dimensions are determined of the parking sensor shell forging, using the finite element analysis. Finally, the parking sensor shell parts are formed by the forging machine under the conditions using finite element analysis. The punch load is close to the simulation result. The dimensions of the experimental forged part agree well with the simulation result and initial design of forged part.

## References

1. M. Markus, K. Markusr, W. Knu, A. Taylan. J. Mater. Proc. Tech. **33** 75 (1992)
2. T. Ishikawa, T. Ishiguro, N. Yukawa, T. Goto. CIRP Annals–Manu.Tech. **63** 289 (2014)
3. Z. Wuhao, H. Xinghui, H. Lin. Proc. Eng. **207** 442 (2017)
4. O. Jensrud, K. Pedersen. J. Mater. Proc. Tech. **80**, 156 (1998)
5. H.M.T. Khaleed, Z. Samad, A.R. Othman, M.A. Mujeebu, A.B. Abdullah, M. M. Zihad. J. Manu. Proc. **13**, 41 (2011)
6. M. Kunogi. J. Sci. Res. Inst. **50**, 215 (1956)
7. C.H. Lee, T. Altan. J. Eng. Indu. **16**, 77 (1972)